Journal of Industrial Microbiology & Biotechnology (2001) 26, 62–69

www.nature.com/jim

^{13}C nuclear magnetic resonance studies on selectively labeled bacterial biofilms†

C Mayer, D Lattner and N Schürks

Institut für Physikalische und Theoretische Chemie, Universität Duisburg, 47048 Duisburg, Germany

Bacterial biofilms of *Pseudomonas aeruginosa* selectively labeled by introduction of 2-^{13}C-glycerol was studied by solid-state and high-resolution nuclear magnetic resonance. The ^{13}C nuclei were mainly integrated into mannuronate and guluronate, the two monomer units forming the bacterial alginate. The signal for the C5 position of the mannuronate, which was easily identified and well separated from other peaks, was analyzed for molecular mobility. The result indicated a high degree of motional freedom within the molecular network of the alginate. Despite the fact that the alginate was part of a solid aqueous gel phase, the reorientation mechanism of the monomer units came close to isotropic tumbling. Solid-state spectra of biofilms labeled in the described manner may serve as a valuable tool for noninvasive analyses of molecular mobility of the alginate component under various influences, thereby revealing important structural information. In addition, the effect of a monovalent electrolyte (LiCl) on the molecular mobility of alginate fragments in an aqueous solution was studied by determining the spin–lattice relaxation times, line widths and line shapes under variations of the ion concentration. The presence of ions accelerated overall motions but left rapid local motions virtually unaffected. *Journal of Industrial Microbiology & Biotechnology* (2001) **26,** 62–69.

Keywords: biofilm; alginate; NMR; solid-state NMR; labeling; molecular dynamics; electrolytes

Introduction

Biofilms grow on practically any surface in a technical or natural environment that permanently or regularly comes into contact with water. The thin slimy layer often found on the surface of rocks in a stream may serve as a well-known example. From a human standpoint, their presence may be either desired or very undesired, depending on the circumstances. Many biotechnological processes rely on localized microorganisms that are immobilized in biofilms. However, in most technical applications, e.g., water processing, biofilms cause severe problems and have to be removed on a regular basis. Biofilms consist of microorganisms temporarily or permanently immobilized in a mixture of polymeric compounds generally referred to as extracellular polymeric substances (EPS) [1,2,4–6]. Polysaccharides, proteins and nucleic acids are typical representatives among the expected EPS constituents. The physical and chemical properties of biofilms are strongly influenced by the composition of extracellular polymers [2,5,6,8,16]. It is believed that the EPS forms a loose network crisscrossing the aqueous environment, leading to the characteristic gel-like macroscopic properties of biofilms [16].

To improve understanding of the biofilm as an ecological structure, it is crucial to analyze its physical state and integral chemical composition as a function of time and of multiple external influences such as shear strength, temperature, or concentration of elementary nutrients. As biofilms are sensitive to destructive sampling, it is desirable to perform analytical studies in a way that guarantees a minimum stress caused by the observation technique.

A method well-known for its noninvasive properties is nuclear magnetic resonance (NMR) spectroscopy. This characteristic advantage of most NMR techniques mainly derives from the low energy and the small absorption coefficient of its radiation. Therefore, NMR has often been used for systematic studies on sensitive biological systems such as biofilms [3,7,10–12,18]. However, this property of NMR spectroscopy is accompanied by its main disadvantage: an extremely low sensitivity. This drawback is especially dramatic in case of the observation of ^{13}C nuclei, which exhibit a quite low natural abundance of approximately 1.1%.

However, this problem may be solved by selective labeling. A relatively simple way to do this is to grow biofilm organisms on media containing ^{13}C-labeled glycerol, which is predominantly used for the biosynthesis of the main polysaccharide component of the EPS, the alginate. This approach also yields simplified spectra, as the labeling is restricted to a given biosynthetic pathway and the observed nucleus is diluted by the presence of numerous surrounding NMR-inactive ^{12}C isotopes. The widths of the individual resonance lines reflect the mobility of the particular molecular environment, wide lines representing relatively slow or sterically hindered reorientation, narrow lines indicating rapid isotropic motion.

In the following, we present NMR results from bacterial biomass generated by *Pseudomonas aeruginosa* in the presence of 2-^{13}C-glycerol under laboratory conditions. This gel-like product produced on agar plates served as a reproducible model of a bacterial biofilm. The spectra and a corresponding method for their numeric analysis demonstrate the potential of ^{13}C NMR for the elucidation of mobility and chemical structure of biofilms under undisturbed (except for mechanical sampling) or controlled conditions. Further, the influence of an electrolyte (LiCl) on the

Correspondence: Dr C Mayer, Institut für Physikalische und Theoretische Chemie, Universität Duisburg, 47048 Duisburg, Germany
†This work was funded by the Deutsche Forschungsgemeinschaft (DFG) as part of the framework of the DFG Research Group "Physical Chemistry of Biofilms."
Received 26 January 2000; accepted 30 August 2000

mobility of dissolved alginate fragments was studied by measurements of relaxation times and spectral line widths under variation of the electrolyte concentration. Structural changes induced by the presence of ions were identified that indicate the presence of strong electrostatic interactions.

Materials and methods

Unlabeled native model biofilm was obtained by growing *P. aeruginosa* SG81 on pseudomonas isolation agar (Difco Inc., Detroit, MI, USA) in petri dishes. The gel-like biomass developing on the surface was mechanically harvested after incubation at 36°C for 24 h.

Labeled native model biofilm was generated by an identical procedure using pseudomonas isolation agar containing 2-^{13}C-glycerol (Cambridge Isotope Laboratories, Andover, MA, USA; 2 g/l) as the main carbon source for polysaccharide biosynthesis.

Samples of isolated and dissolved alginate were obtained from the model biofilm by a standard procedure described by Grobe *et al.* [9]. The bacterial growth from approximately 20 agar plates was harvested and dispersed in a sterile solution of NaCl (0.14 M, 100 ml). The suspension was treated in a laboratory centrifuge at 10°C, applying 20,000×*g* for 1 h, then 40,000×*g* for 2 h. The resulting clear solution was separated and added to 300 ml ethanol at 0°C and stirred for 30 min, causing the alginate to precipitate. The alginate was removed by filtration and washed several times with fresh ethanol. The product was dried and redissolved either in deionized water or in an aqueous solution of lithium chloride of a given concentration to yield a final alginate content of 10 g/l.

NMR measurements on samples in the gel state were performed on a solid-state spectrometer (ASX 400, Bruker, Karlsruhe, Germany) under static conditions in a modified 10-mm probe. All spectra were proton decoupled and were accumulated in 4000 scans with a delay time of 3 s. A ^{13}C pulse duration of 7 μs was applied for the single 90° pulse used for each scan. Line widths were determined as "full widths at half height," spin–lattice relaxation times were measured experimentally by saturation recovery pulse sequences.

For corresponding high-resolution NMR experiments, the redissolved alginate was partially degraded by acidic hydrolysis (2 h at 100°C in 1 M HCl) generally following the procedure described by Grasdalen *et al.* [8]. The NMR measurement was performed on a high-resolution DRX 500 spectrometer (Bruker) at 60°C under proton decoupling.

Results

The result of a direct examination of unlabeled native model biofilm from *P. aeruginosa* by ^{13}C NMR is shown in Figure 1. Except for two sharp signals corresponding to the residual glycerol content of the cultivating medium, all peaks exhibit a relatively poor signal-to-noise ratio. The signal near 180 ppm indicates the presence of carbonyl groups and a number of peaks between 10 and 50 ppm derive from hydrocarbon residues. Wide spectral line shapes (e.g., at 175 ppm) coexist with narrow ones (mainly between 10 and 80 ppm). Further signal assignments are difficult if not impossible.

The situation changed completely when the biomass was grown on medium containing labeled glycerol (^{13}C in the central carbon position). A spectrum of the native model biofilm developing under these conditions is shown in Figure 2. Several strong peaks are present between 60 and 80 ppm chemical shift whereas the weak signal at 175 ppm remains. The lines between 60 and 80 ppm vary significantly in their spectral width: although most of the signals exhibit line widths around 1 ppm, a corresponding value of approximately 3 ppm is detected for a single peak near 80 ppm.

To positively identify signals that belong to the main polysaccharide constituent of the EPS, alginate was isolated by the procedure described in the experimental section. The alginate fraction was then degraded into small soluble units that were mobile

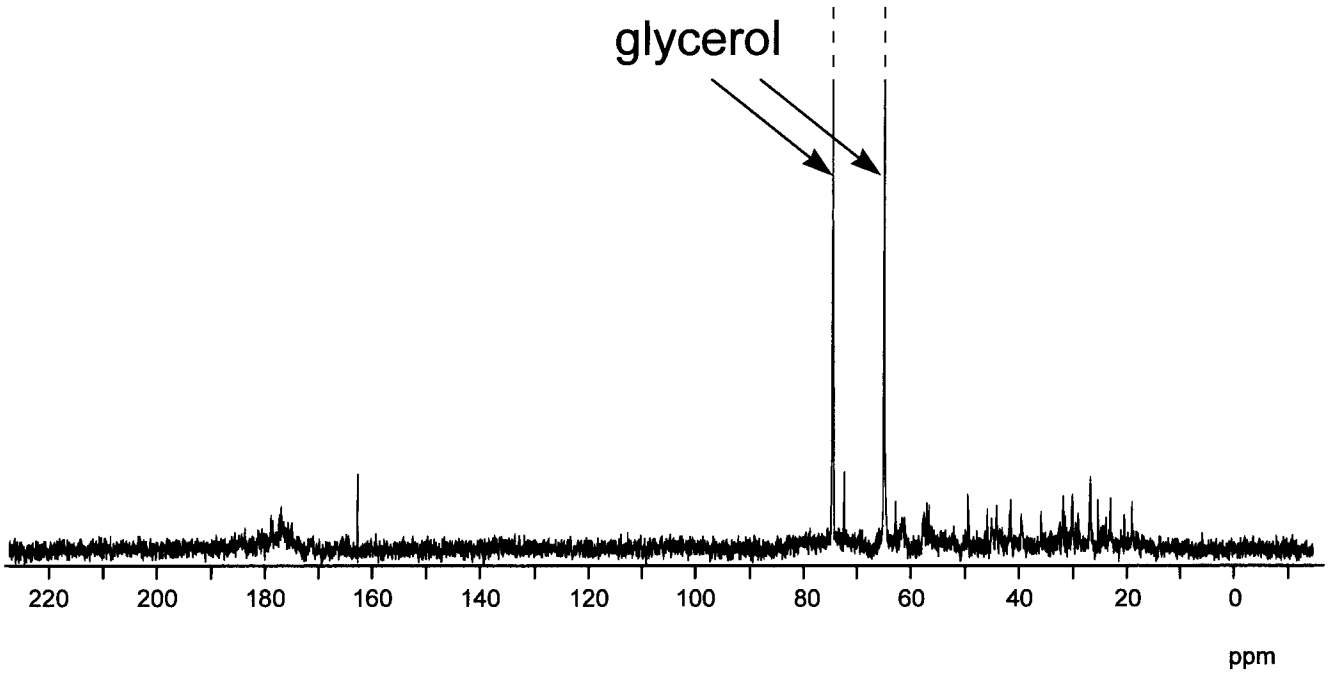

Figure 1 Proton decoupled ^{13}C NMR spectrum of unlabeled native biofilm of *P. aeruginosa*. Except for the peaks of residual unlabeled glycerol, all signals exhibit poor signal-to-noise ratios.

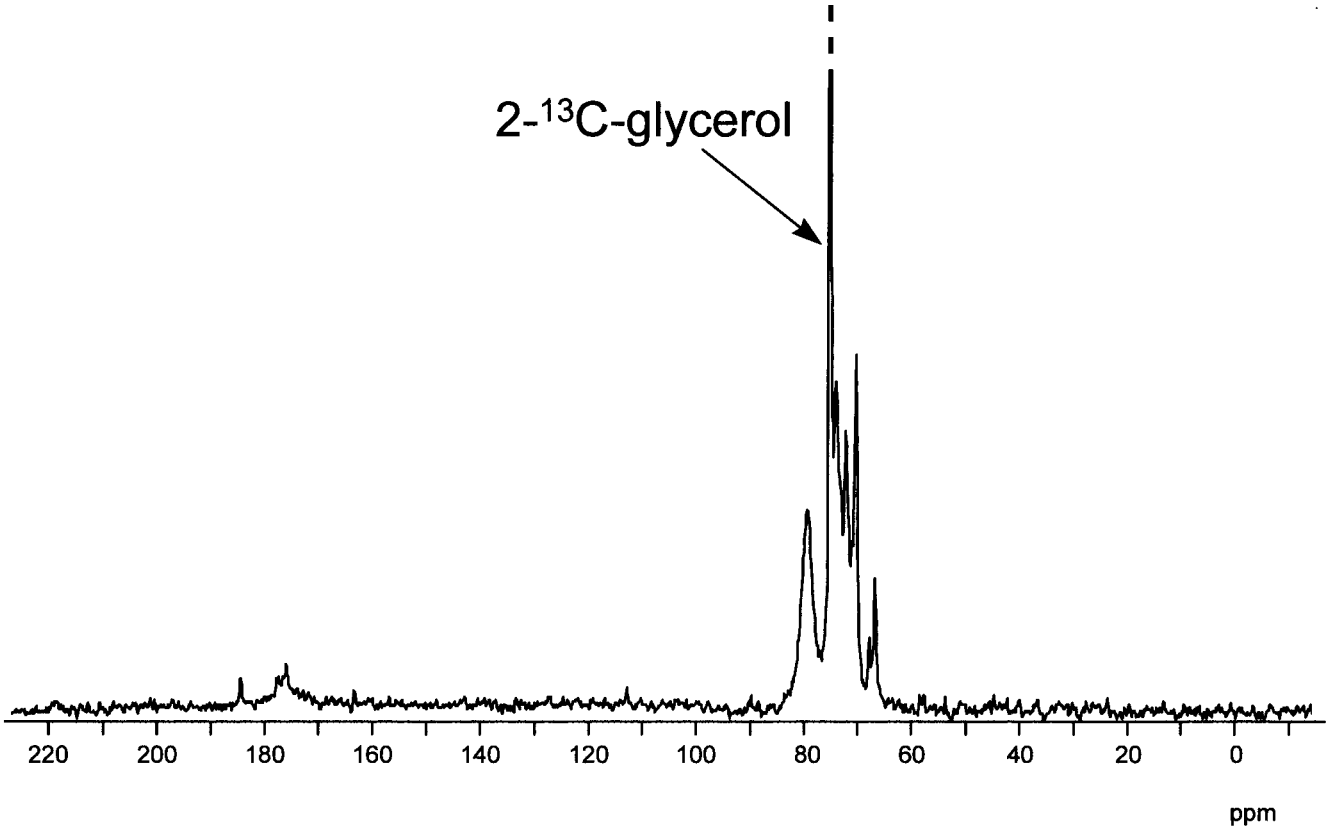

Figure 2 Proton decoupled ^{13}C NMR spectrum of native biofilm of *P. aeruginosa* grown in the presence of 2-^{13}C-glycerol. All detectable signals represent labeled carbon positions. Except for the peak at 75 ppm, which indicates residual labeled glycerol, the spectrum is dominated by constituents of the extracellular polymeric substances, especially the alginate.

enough to yield a high-resolution spectrum. The resulting spectrum is shown in Figure 3 in comparison with a corresponding spectrum of unlabeled alginate.

So far, the model biofilm has been studied under relatively noninvasive conditions, except for the process of mechanical harvesting, which should not lead to changes in its molecular structure. To study the effect of an electrolyte on molecular interactions within the alginate, it was necessary to disrupt the macromolecular network and dissolve the alginate fragments in the presence of various ion concentrations. As an example for a monovalent electrolyte, an aqueous solution of LiCl at concentrations between 0.01 and 2.5 mol/l was chosen.

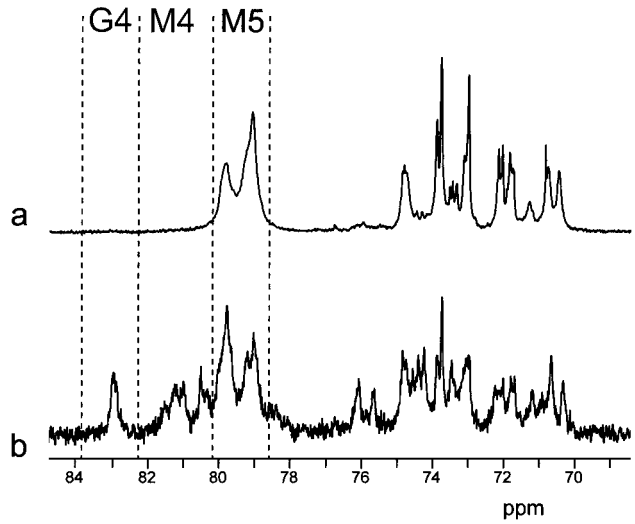

Figure 3 Comparison between proton decoupled high-resolution ^{13}C NMR spectra of isolated and partially degraded alginates from (a) selectively labeled, and (b) unlabeled cultures of *P. aeruginosa*. The spectrum (a) of the labeled alginate fragments contains a distinct fraction of the peaks visible in spectrum (b).

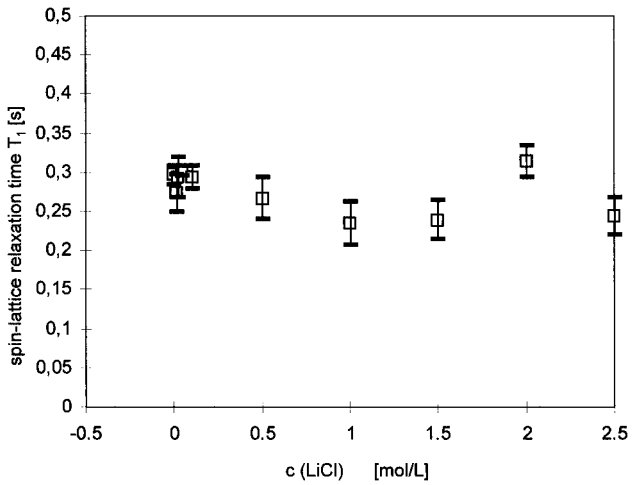

Figure 4 Spin–lattice relaxation times T_1 of an aqueous alginate solution as a function of the LiCl concentration. The values have been determined on the ^{13}C signal near 80 ppm applying a saturation recovery pulse sequence and the experimental uncertainty is indicated by error bars.

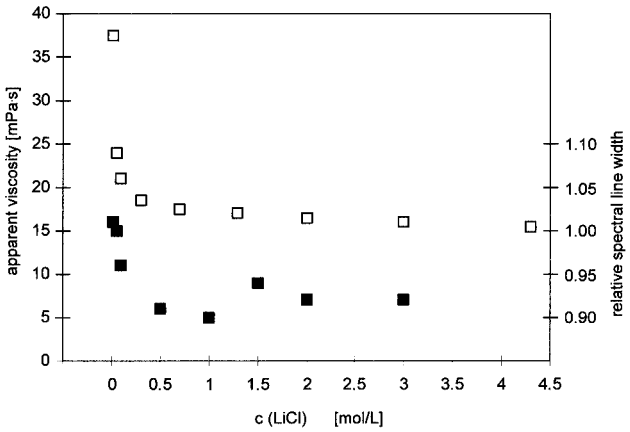

Figure 5 Full symbols: spectral line width of the ^{13}C signal near 80 ppm of an aqueous alginate solution as a function of the LiCl concentration. The values are normalized to the line width determined in the absence of LiCl. Open symbols: apparent solution viscosities as a function of the LiCl concentration measured independently by a rotating couette viscometer [17].

The effect of various concentrations of LiCl on the spin–lattice relaxation of the peak at 80 ppm is represented in Figure 4. Within the given experimental error, the observed variation of the spin–lattice relaxation time T_1 does not show a significant tendency with increasing ion concentration. Except for a single elevated point at 2 mol/l, the values of T_1 may be considered constant for the full concentration range.

The situation is different for the spectral line widths (Figure 5, solid symbols). All line widths given were determined on the signal near 80 ppm with an experimental error smaller than 3%. In this case, a clear tendency was observed for ion concentrations between 0 and 1 mol/l, the normalized line width (the observed line width divided by the original line width in the absence of electrolyte) decreasing with increasing ion concentration. At concentrations above 1 mol/l, the values level out near a normalized relaxation rate of 0.9. In Figure 5, the dependency of the line width is compared with the apparent viscosity of the solution as determined by a rotating couette viscometer [16,17]. The corresponding NMR line shapes for six selected concentrations are shown in Figure 6, left column. In addition to the decrease in line width, a subtle change in

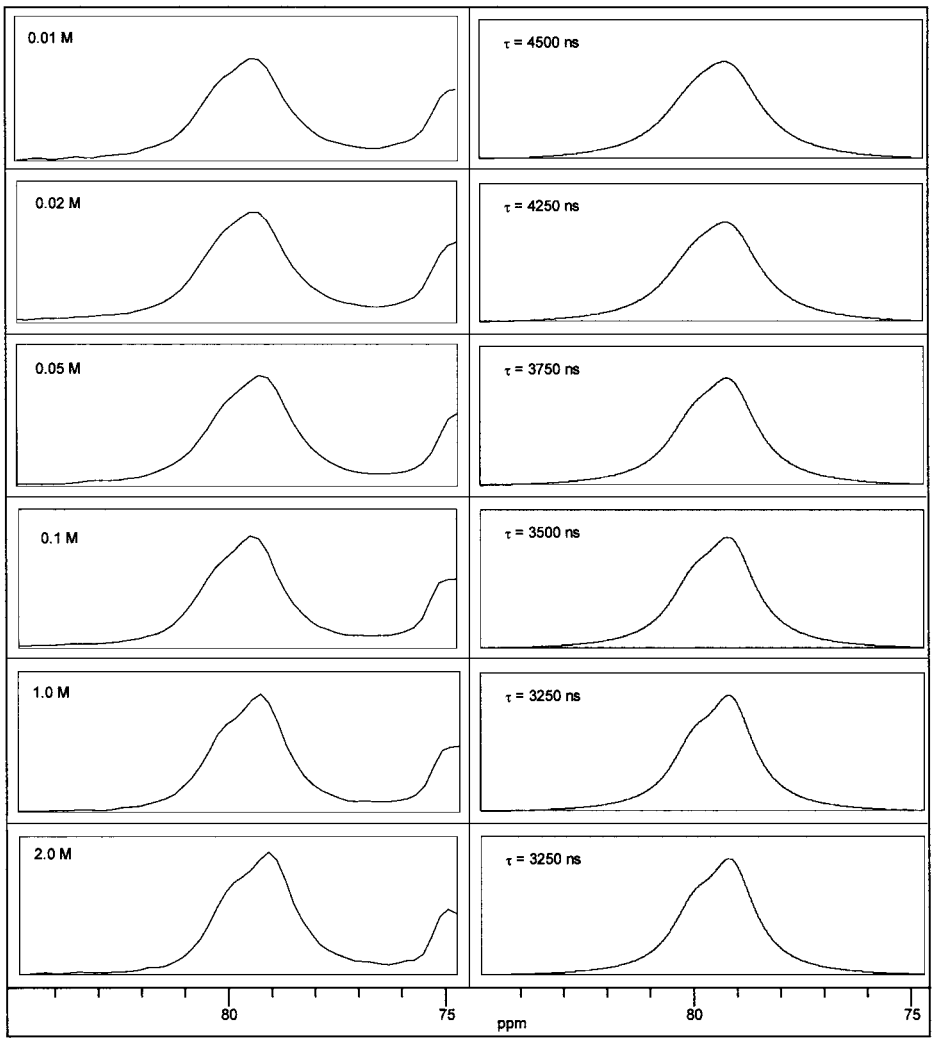

Figure 6 Experimental (left column) and simulated (right column) spectral line shapes of the ^{13}C signal near 80 ppm at different concentrations of LiCl. The calculations are based on an isotropic rotational diffusion with the tensor data given in the text. The correlation times τ for the resulting best fits are given for each spectrum.

the shape of the resonance line is observed with increasing ion concentration. At concentrations above 0.1 mol/l, a shallow dip appears at 79.5 ppm near the top of the peak.

Discussion

The chemical composition of the extracellular material from *P. aeruginosa* SG 81 has been studied in detail. Its main polymer constituents are carbohydrates, but it also contains protein (approximately 4.3% with respect to the carbohydrate content) [9]. Other biopolymers such as polynucleotides or lipoproteins are likely to be present as well [5]. Alginate, the main polysaccharide of *P. aeruginosa*, consists of guluronate (28%) and mannuronate (72%) units, the latter being partially acetylated (Figure 7). Poly-guluronate blocks are absent and poly-mannuronate blocks are usually short (unpublished results).

As expected, the ^{13}C NMR experiment on the unlabeled biofilm yielded poor results. The only information that may be derived from the spectrum in Figure 1 may be summarized as follows: (a) solid-state components coexist with a mobile phase indicated by the simultaneous existence of wide and narrow lines in the spectrum, (b) numerous lines between 10 and 50 ppm chemical shift indicate the presence of various hydrocarbon residues and (c) a wide line near 175 ppm represents carbonyl groups of solid or motionally hindered constituents.

After selective spin labeling, the spectrum of native biofilm was of significantly better quality (Figure 2). All signals corresponding to labeled carbon positions appear strongly enhanced. Among them, the C2 position of the glycerol (at 75 ppm) and the carbonyl positions (170–180 ppm) are easily identified from the original spectrum. The most interesting feature, however, is represented by a wide peak near 80 ppm. In contrast to the other signals in the vicinity of 70 ppm, it obviously derives from a molecular environment with restricted mobility, as its outlines reflect an almost ideal Lorentzian line shape with significantly increased spectral width of approximately 3 ppm. Since it is sufficiently separated from other peaks, it is well suited for a detailed line shape analysis. However, its assignment becomes a necessary precondition for further interpretation of the data.

Grasdalen *et al.* [8] assigned the various signals in ^{13}C NMR spectra of partially degraded alginate to the various carbon positions of mannuronate and guluronate, the monosaccharides that represent its monomeric units (Figure 7). Based on these data, the comparison between spectra of labeled and unlabeled partially degraded alginates (Figure 3, top and bottom) allows an easy identification of the labeled carbon positions. Three groups of signals between 84 and 78 ppm in spectrum b can be clearly

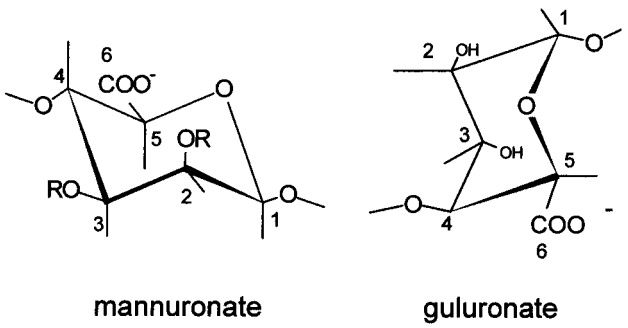

Figure 7 Molecular structures of the two characteristic monomer units (mannuronic acid, left, and guluronic acid, right) of an alginate macromolecule. In case of bacterial alginate, the mannuronate units may be partially acetylated.

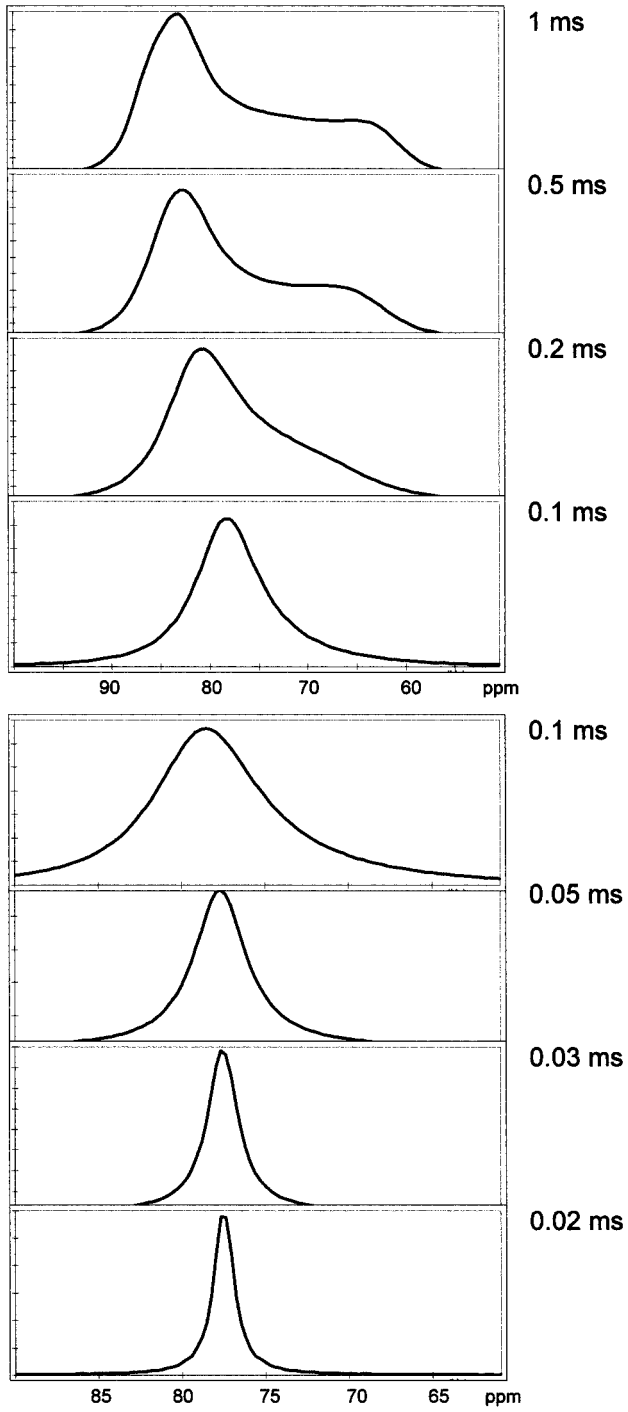

Figure 8 Simulated ^{13}C NMR spectra for an isotropic tumbling motion with various correlation times (1–0.1 ms, and 0.1–0.02 ms with expanded horizontal scaling). All calculations are based on a chemical shift anisotropy similar to the inner carbon atoms of ammonium tartrate ($\sigma_{11} = \sigma_{iso} + 13$ ppm, $\sigma_{22} = \sigma_{iso} + 7$ ppm, $\sigma_{33} = \sigma_{iso} - 20$ ppm), which carry a set of chemical residues either identical or comparable to carbon position 5 in the mannuronate residue.

assigned to three carbon positions of the monomer units of the alginate chain: the C4 position of guluronate (G4), the C4 position of mannuronate (M4) and the C5 position of mannuronate (M5). The peaks at 79.1 and 79.8 ppm in spectrum a therefore derive from the C5 position of mannuronate, which obviously is one of the labeled positions (Figure 3, top).

To analyze the reorientation process responsible for its (incomplete) averaging, a numerical simulation procedure for NMR spectra [13,14] is applied. Basic assumptions necessary for numerical calculation of the signal near 80 ppm are discussed in the following.

It is generally accepted that the source of line broadening for proton decoupled ^{13}C NMR spectra is merely represented by the chemical shift anisotropy [19]. The two averaged chemical shifts for the relevant carbon position ($\sigma_{iso(1)}$=79.1 ppm, 70% and $\sigma_{iso(2)}$=79.8 ppm, 30%) are abstracted from the two corresponding signals in the high-resolution spectrum (Figure 3). The anisotropy of the chemical shift tensor is completely described by a set of characteristic parameters σ_{11}, σ_{22}, and σ_{33}. For the following calculations, we use values similar to those that have been determined for the inner carbon atoms of ammonium tartrate ($\sigma_{11}=\sigma_{iso}+13$ ppm, $\sigma_{22}=\sigma_{iso}+7$ ppm, $\sigma_{33}=\sigma_{iso}-20$ ppm) [20], which carry a set of chemical residues that are either identical or comparable to those of the C5 position of the mannuronate unit in the alginate. The resulting chemical shift anisotropy tensors $\sigma_{(1)}$ ($\sigma_{(1)11}$=92.1 ppm, $\sigma_{(1)22}$=86.1 ppm, $\sigma_{(1)33}$=59.1 ppm) and $\sigma_{(2)}$ ($\sigma_{(2)11}$=92.8 ppm, $\sigma_{(2)22}$=86.8 ppm, $\sigma_{(2)33}$=59.8 ppm) are weighted by the estimated relative intensities of the two peaks (70% for $\sigma_{(1)}$, 30% for $\sigma_{(2)}$). The overall interaction tensor $\sigma_{(total)}=0.7\,\sigma_{(1)}+0.3\,\sigma_{(2)}$ is in accordance with a spectrum of the dry, solid, and therefore rigid material (not shown).

The observed carbon atom is expected to be part of the loose EPS network, therefore its local reorientation should be restricted by steric hindrance. However, the shape of the observed signal strongly indicates a motion that leads to a very efficient tensor averaging, since the NMR signal appears totally symmetric and lacks all characteristics of a residual powder pattern. Consequently, it is justified to postulate isotropic rotational diffusion as an approximation for the motional mechanism.

Based on the assumed dynamic process and the given anisotropy of the chemical shift, model calculations were performed that demonstrated the sensitivity of the spectral line shape with respect to the time scale of the motion (Figure 8). Under variation of the motional correlation time and based on the interaction tensor $\sigma_{(total)}$, the simulated line shape was carefully fitted to the experimental carbon signal (Figure 9). The best fit is found for a correlation time for the isotropic rotational diffusion of 30 μs. This corresponds to a relatively rapid motion and supports the idea of the

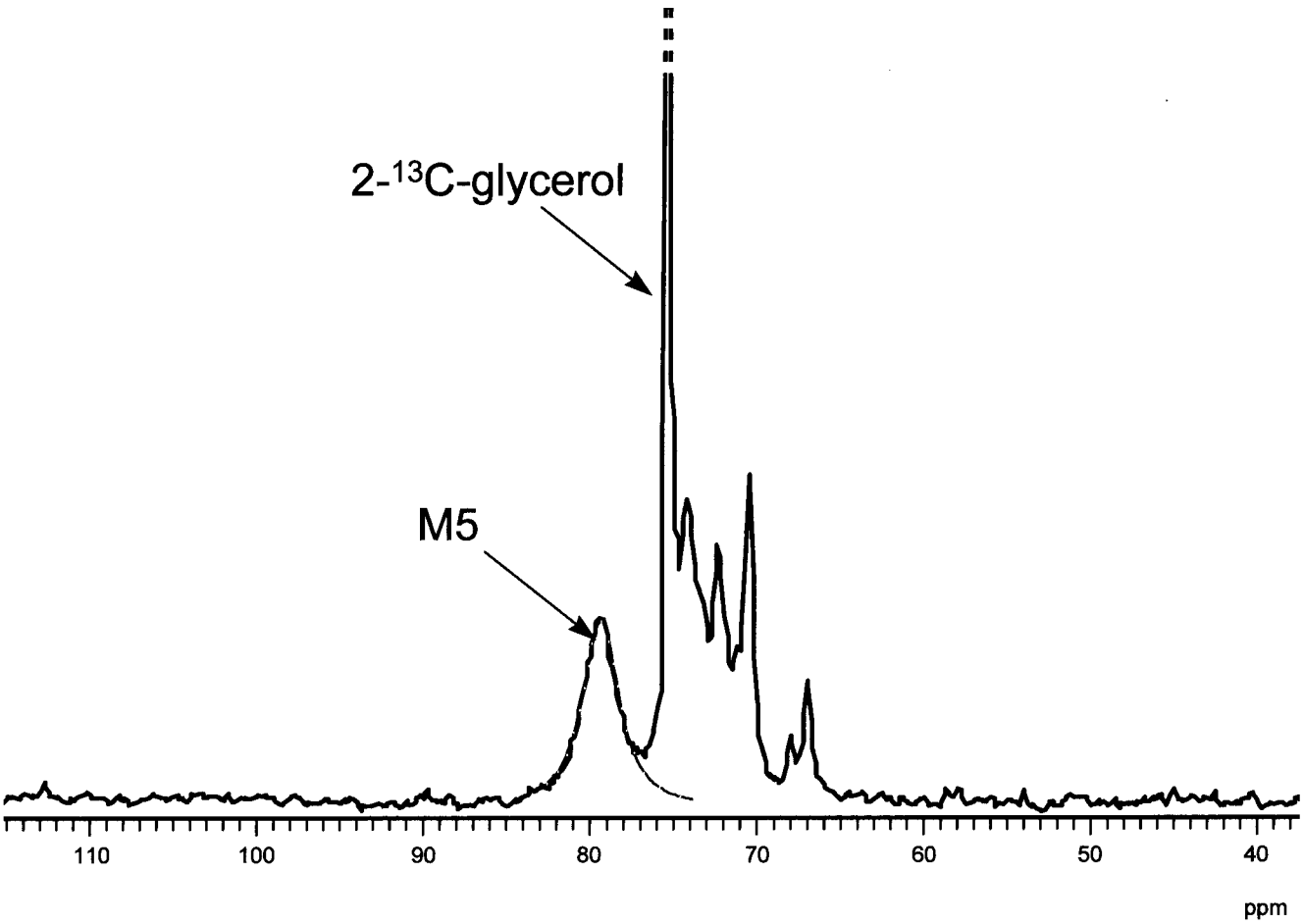

Figure 9 Expanded fraction of the ^{13}C spectrum of labeled alginate shown in Figure 2. The broken line in the region between 74 and 84 ppm represents the calculated best fit for the ^{13}C signal of the C5 position in mannuronate units. The result is based on an isotropic tumbling motion with a correlation time of 30 μs and the estimated interaction tensor described in the text.

EPS forming a loose framework with a high degree of internal dynamics. It is very likely that these dynamics are strongly influenced by the presence of electrolytes as has been detected earlier for comparable model systems [15,16].

With the high degree of sensitivity of the spectral results with respect to the characteristics of molecular mobility, the ^{13}C NMR signal presents a perfect indicator for inter- and intramolecular motions and local interactions of the polysaccharide chains in the EPS. It is therefore expected that corresponding studies of the mobility of the carbohydrate component under the influence of electrolytes and other chemical conditions will shed more light on the microscopic structure of the material that represents the main structural element of biofilms. However, to assure a well-defined and homogeneous concentration of the added chemical throughout the sample, we presently prefer to work on alginate solutions rather than on the original model biofilm. Therefore, the effect of a lithium chloride solution on the NMR signal has been studied on a homogenized aqueous solution of the alginate, data are shown in Figures 4–6.

The observed dependence of the spin–lattice relaxation time on the ion concentration (Figure 4) was weak and, compared to the experimental error, negligible. As the spin–lattice relaxation is sensitive to motions in the megahertz range such as local isomerizations, one can state that local motions, e.g., motions of single HCOH units, are not significantly affected by the presence of anions or cations. This is in accordance with observations on polyacrylic acid as a typical polyelectrolyte [15,16]. Even if ions have an influence on the local environment of single carbon units, this is only relevant for a very small portion of all carbon positions.

The situation differs significantly for the observable spectral line width. The features of the line shape are sensitive to much slower motions in the kilohertz regime, such as reorientations of the whole molecule or of large sections of the alginate chain. The dependence shown by the closed symbols in Figure 5 is indicative of a detectable change of mobility when the ion concentration is increased from 0.01 to 1 mol/l. The shape of the plot shows some similarity with corresponding data on the apparent viscosity of the solution [16,17] (open symbols). This indicates that the mechanism mainly responsible for the line widths is represented by the isotropic diffusion of the dissolved alginate particles, which is directly connected to the viscosity of the solution. A corresponding numeric simulation based on isotropic rotational diffusion and the tensor elements discussed above yields spectra that are very similar to the experimental line shapes (Figure 6). With correlation times between 3.25 and 4.5 μs, the effective motional mechanism for the dissolved alginate fragments is much faster than the chain motion with a time constant of 30 μs, which has been identified for the solid alginate. The slow chain motion may therefore be neglected for the alginate fragments, all spectral simulations take account of the isotopic tumbling only. The dependence of the resulting correlation times on the ion concentration again resembles the one for apparent viscosity of the solution (Figure 10). The most plausible explanation for acceleration caused by the presence of the electrolyte is a structural change induced by electrostatic interactions [15,16]. At low ion concentrations, the repulsive forces between the negative charges on the alginate chain force the molecule into long, stretched shape, inducing a high viscosity and wide NMR signals. On addition of ions, the charges become partially compensated, leading to reduced electrostatic interactions within the chain and to the formation of a compact random coil. Consequently, the solution viscosity is lowered and the width of NMR signals is decreased. This is in accordance with earlier results on EPS solution [15–17] where the repulsive electrostatic interactions have been identified as important forces, which determine mechanical properties of biofilms.

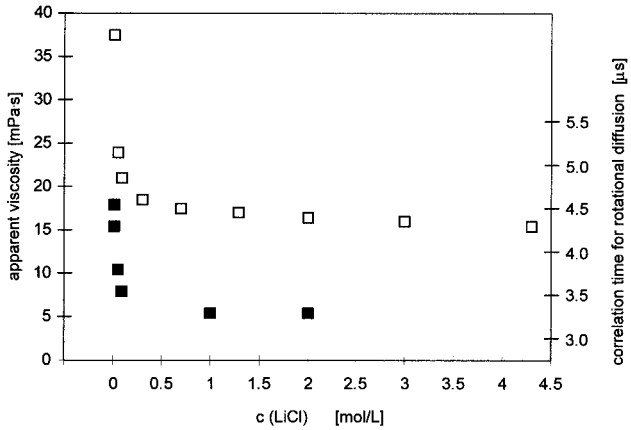

Figure 10 Correlation times for an isotropic rotational diffusion of alginate molecules as a function of the LiCl concentration (full symbols). The correlation times derive from simulated spectra fitted to the ^{13}C signal near 80 ppm (see Figure 6). Values for the apparent viscosity of the alginate solution (open symbols) are shown for comparison.

Acknowledgements

We thank H.-C. Flemming, J. Wingender and their coworkers for laboratory space, valuable practical assistance and many helpful discussions.

References

1 Christensen BE. 1989. The role of extracellular polysaccharide biofilms. *J Biotechnol* 10: 181–202.
2 Christensen BE and WG Characklis. 1990. Physical and chemical properties of biofilms. In: Characklis WG and KC Marshall (Eds.), Biofilms. Wiley, New York, pp. 93–130.
3 Clark DS. 1990. Noninvasive techniques in studies of immobilized cells. In: Bont JAM de, J Visser, B Mattiasson and J Tramper (Eds.), Physiology of Immobilized Cells. Elsevier, Amsterdam, pp. 603–613.
4 Cooksey KE. 1992. Extracellular polymers in biofilms. In: Melo LF, MM Fletcher and TR Bott (Eds.), Biofilms: Science and Technology. Kluwer Academic Publishers, Dordrecht, pp. 137–147.
5 Flemming HC, J Wingender and C Mayer. 1998. Extracellular polymeric substances — the material which forms the biofilm. *Meded — Fac Landbouwkd Toegepaste Biol Wet* 63: 1129.
6 Flemming HC, J Wingender, R Moritz, W Borchard and C Mayer. 1999. Physico-chemical properties of biofilms — a short review, p. 1. In: Keevil CW, C Dow, A Godfree and D Holt (Eds.), Biofilms in the Aquatic Environment. Royal Society of Chemistry, Cambridge.
7 Gladden LF. 1994. Nuclear magnetic resonance in chemical engineering — principles and applications. *Chem Eng Sci* 49 (20): 3339–3408.
8 Grasdalen H, B Larsen and O Smidsrød. 1981. ^{13}C-N.M.R. studies of monomeric composition and sequence in alginate. *Carbohydr Res* 89: 179–191.
9 Grobe S, J Wingender and HG Trüper. 1995. Characterization of mucoid *Pseudomonas aeruginosa* strains isolated from technical water systems. *J Appl Bacteriol* 79: 94–102.
10 Lewandowski Z, SA Altobelli and E Fukushima. 1993. NMR and microelectrode studies of hydrodynamics and kinetics in biofilms. *Biotechnol Prog* 9 (1): 40–45.

11 Lewandowski Z, SA Altobelli, PD Majors and E Fukushima. 1992. NMR imaging of hydrodynamics near microbially colonized surfaces. *Water Sci Technol* 26: 577–584.
12 Lohmeier-Vogel EM, DD McIntyre and HJ Vogel. 1990. Nuclear magnetic resonance spectroscopy as an analytical tool in biotechnology. In: Bont JAM de, J Visser, B Mattiasson and J Tramper, (Eds.), Physiology of immobilized cells. Elsevier, Amsterdam, pp. 661–676.
13 Mayer C. 1999. Lineshape calculations on spreadsheet software. *J Magn Reson* 138 (1): 1–11.
14 Mayer C. 1999. Calculation of MAS spectra influenced by slow molecular tumbling. *J Magn Reson* 139 (1): 132–138.
15 Mayer C. 2000. NMR on bacterial biofilms and model systems. In: Barbotin JN and JC Portais (Eds.), NMR in Microbiology. Horizon Scientific Press, Wymondham, pp. 363–379.
16 Mayer C, R Moritz, C Kirschner, W Borchard, J Wingender and HC Flemming. 1999. Intermolecular interactions in biofilms: studies on bacterial biofilms and model systems. *Int J Biol Macromol* 26 (1): 3–16.
17 Moritz R. 1997. Viskositätsmessungen an Biofilmen: analyse von intermolekularen Wechselwirkungen. Diploma thesis, University of Duisburg, Germany.
18 Neu TR, T Dengler, B Jann and K Poralla. 1992. Structural studies of an emulsion-stabilizing exopolysaccharide produced by an adhesive, hydrophobic *Rhodococcus* strain. *J Gen Microbiol* 138: 2531–2537.
19 Slichter CP. 1978. Principles of Magnetic Resonance. Springer Verlag, Berlin, pp. 82ff.
20 Veeman WS. 1984. Carbon-13 chemical shift anisotropy. *Prog Nucl Magn Reson Spectrosc* 16: 193–235.